

## Discs and Planetary Formation

J. C. B. Papaloizou

*Astronomy Unit, Queen Mary & Westfield College  
Mile End Road, London E14NS, UK*

C. Terquem

*Lick Observatory, University of California  
Santa Cruz, CA 95064, USA*

R. P. Nelson

*Astronomy Unit, Queen Mary & Westfield College  
Mile End Road, London E14NS, UK*

**Abstract.** The formation, structure and evolution of protoplanetary discs is considered. The formation of giant planets within the environment of these models is also discussed.

### 1. Introduction

The hypothesis that the planets in the solar system were formed in a flattened differentially rotating gaseous disc was originally proposed by Laplace (1796). The suggestion arises naturally in view of their orbital configuration. They are in near circular orbits which approximately lie in the same plane. Models in which planet formation occurs in gaseous discs have been the subject of much theoretical interest in recent times (e.g. Lin & Papaloizou 1985, 1993 and references therein).

When discussing the large scale physical properties of such a disc, it is convenient to make the idealization that it is infinitesimally thin or completely flat. When, as in the present solar system, most of the mass lies in a central star of mass  $M_*$ , the local gravitational acceleration can be taken to be  $g = GM_*/r^2$ . A gaseous element at radius  $r$  then rotates in circular orbit with angular velocity  $\Omega$ , which, to a good approximation, is obtained from centrifugal balance by equating  $g = r\Omega^2$ . This gives Kepler's law

$$\Omega^2 = \frac{GM_*}{r^3}. \quad (1)$$

In this approximation, in which forces other than that due to the gravity of the central star are neglected, material rotates conserving its specific angular momentum  $j = r^2\Omega$ . This then changes only slowly when viscous or other perturbative forces are taken account of.

### 1.1. Observations of protostellar discs

Between 25 and 75 percent of young stellar objects in the Orion nebula appear to have discs (McCaughrean & Stauffer 1994). Masses of  $\sim 10^{-2\pm 1} M_{\odot}$ , and dimensions  $\sim 40 \pm 20$  AU have been estimated (Beckwith & Sargent 1996). The presence of discs on the scale of astronomical units has been inferred from the infrared excesses observed in about half of all T Tauri stars. Their colors and magnitudes can be fitted by those expected for young pre-main sequence stars with ages  $\sim 10^6$  yr (Strom et al. 1993). The infrared emission may be produced by the gravitational potential energy liberated by matter flowing inwards at a rate  $\dot{M} \sim 10^{-8\pm 1} M_{\odot} \text{ yr}^{-1}$ . The non observation of discs around older T Tauri stars together with these values of  $\dot{M}$  suggest a disc lifetime of  $\sim 10^7$  yr.

### 1.2. Formation of discs

It is believed that protostars and protoplanetary discs derive from interstellar matter contained in molecular clouds. Observations (Goodman et al. 1993) indicate that typical star-forming dense cores in dark molecular clouds have specific angular momentum  $j > 6 \times 10^{20} \text{ cm}^2 \text{ s}^{-1}$ . When these clouds undergo gravitational collapse,  $j$  is initially approximately conserved because the collapse is dynamical. Gas in the outer parts will not be able to fall directly to the centre ( $r = 0$ ) if  $j$  is not zero.

To obtain an estimate of the initial size of the disc, we consider the idealized situation when the pre-collapse cloud is a cold rotating sphere of mass  $M$  and radius  $R$ , with a single axis of rotation. Matter located on the rotation axis has no angular momentum so it can fall directly to the centre. An estimate of the time required,  $t_{ff}$ , is given by the time required to free fall from rest through a distance  $R$  under the initial inward gravitational acceleration at the surface,  $g = GM/R^2$ . This gives  $t_{ff} = \sqrt{2R/g} = \sqrt{2R^3/(GM)}$ . In terms of the initial mean density  $\bar{\rho}$  of the cloud,  $t_{ff} = \sqrt{3/(2\pi G\bar{\rho})}$ . For a cloud core with  $M = 1 M_{\odot}$  and  $R = 0.1$  pc, this gives  $t_{ff} \sim 6 \times 10^5$  yr.

While matter located on the rotation axis can move directly to the centre, matter in the equatorial plane at the surface of the sphere will be at the outermost radius  $R_d$  of a disc after collapse. Conservation of specific angular momentum determines  $R_d$ . Assuming the total mass,  $M$ , to be concentrated at the centre, the angular velocity at the outer edge of the disc will be given by Kepler's law such that

$$\Omega^2 = \frac{j^2}{R_d^4} = \frac{GM}{R_d^3}. \quad (2)$$

Thus  $R_d$  is given in terms of the conserved quantities  $j$  and  $M$  by  $R_d = j^2/(GM)$ . Adopting  $j = 6 \times 10^{20} \text{ cm}^2 \text{ s}^{-1}$  and  $M = 1 M_{\odot}$ , we find that  $R_d \sim 180$  AU. The characteristic dimension of such a disc is about an order of magnitude larger than our present solar system but is similar to those of protostellar discs now being observed by direct imaging.

## 2. Early evolution

The formation of a protostellar disc through the collapse of a molecular cloud core takes  $10^5$ – $10^6$  yr. During the early stages when the disc is still embedded

(class 0/1 object) and has a significant mass compared to the central star, there may exist strong disc winds and bipolar outflows (e.g. Reipurth et al. 1997) with associated magnetic fields. During this stage a hydromagnetic disc wind may be an important means of angular momentum removal for the system (see Papaloizou & Lin 1995, and references therein).

When the mass of the disc is significant compared to that of the star, there may be a short period ( $\sim 10^5$  yr) of non axisymmetric global gravitational instability with associated outward angular momentum transport (Papaloizou & Savonije 1991; Heemskerk et al. 1992; Laughlin & Bodenheimer 1994; Pickett et al. 1998) that results in additional mass growth of the central star. This redistribution may occur on the dynamical timescale (a few orbits) of the outer part of the disc and so may be quite rapid, on the order of  $10^5$  yr for  $R = 500$  AU. The parameter governing the importance of disc self-gravity is the Toomre parameter,  $Q = M_* H / (M_d r)$ , with  $M_d$  being the disc mass contained within radius  $r$  and  $H$  being the disc semi-thickness. In this review we shall take  $H$  to be the distance between the disc mid-plane and surface. This is usually a factor of 2–3 larger than the vertical extent reached by a disc particle moving through the disc mid-plane with the local sound speed  $c_s$ . Thus  $H \sim (2c_s) / \Omega$ . Typically  $H/r \sim 0.1$  (Stapelfeldt et al. 1998) such that the condition for the importance of self-gravity,  $Q \sim 1$ , gives  $M_d \sim 0.1 M_*$ .

The characteristic scale associated with growing density perturbations in a disc undergoing gravitational instability with  $Q \sim 1$  is  $\sim H$ , and the corresponding mass scale is  $M_d (H/r)^2 \sim M_* (H/r)^3$ , which is  $\sim 1 M_J$  for  $H/r \sim 0.1$  and  $M_* = 1 M_\odot$ , with  $M_J$  being Jupiter’s mass. Gravitational instability does not necessarily lead to fragmentation (e.g. Pickett et al. 1998), nonetheless it has been proposed as a mechanism for directly forming giant planets by Cameron (1978) and more recently by Boss (1998).

During the period of global gravitational instability, it is reasonable to suppose that the disc mass is quickly redistributed and reduced such that global gravitational stability is restored ( $Q > 1$ ), after which further disc evolution occurs on a longer timescale governed by viscosity with effects due to self-gravity being small.

## 2.1. Viscous evolution

During this phase, the disc may attain a configuration similar to that expected for the minimum mass primordial solar nebula,  $M_d \sim 10^{-2} - 10^{-1} M_\odot$ . Planets have been proposed to form out of such a disc by a process of growth through planetesimal accumulation followed, in the giant planet case, by gas accretion (Safronov 1969; Wetherill & Stewart 1989).

During this evolutionary phase, it is reasonable to regard the disc as an axisymmetric configuration in which, to a first approximation, material orbits in circular Keplerian orbits. However, other weaker forces due to internal pressure, viscosity, or magnetic fields may also operate in the disc. These can result in angular momentum redistribution on a long timescale. In order to flow inwards, material has to transport its angular momentum outwards to matter at larger radii. The angular momentum transport process determines the timescale on which mass accretion can occur and hence the evolutionary timescale of the disc.

Historically, the first angular momentum transport mechanism to be considered was through the action of viscosity (von Weizsäcker 1948). This acts through the friction of neighbouring sections of the disc upon each other. The inner regions rotate faster than the outer regions and thus viscous friction tends to communicate angular momentum from the inner parts of the disc to the outer parts. In order to result in evolution on astronomically interesting timescales, it is necessary to suppose that an anomalously large viscosity is produced through the action of some sort of turbulence. The magnitude of the viscosity is usually parameterized through the Shakura & Sunyaev (1973)  $\alpha$  prescription.

In this we suppose the kinematic viscosity coefficient  $\nu = \alpha c_s^2 / \Omega \sim \alpha H^2 \Omega$ , where  $\alpha$  is a dimensionless constant which must be less than unity. Currently the most likely mechanism for producing turbulence is through hydromagnetic instabilities (Balbus & Hawley 1991) which might produce  $\alpha \sim 0.01$ , provided the disc has adequate ionization.

Gammie (1996) has proposed a model in which viscosity only operates in the surface layers where external sources of ionization such as cosmic rays can penetrate. Such layered models may have an interior dead zone of material for  $r > 0.1$  AU and, although they can be considered as models with a variable  $\alpha$ , they will behave somewhat differently from the standard models considered here which have  $\alpha$  assumed to be constant throughout.

### 3. The diffusion equation for disc evolution

The evolution of a viscous disc is controlled by angular momentum conservation. The conservation of specific angular momentum may be expressed in the form (eg. Papaloizou & Lin 1995)

$$\rho \frac{Dj}{Dt} = -\nabla \cdot \mathbf{F} = -\frac{1}{r} \frac{\partial}{\partial r} (r F_r) - \frac{\partial}{\partial z} (F_z), \quad (3)$$

where  $\mathbf{F} = (F_r, F_z)$  is the angular momentum flux, with the vertical coordinate being denoted by  $z$ , and  $\rho$  is the mass density.

The process of vertical averaging applied to equation (3) in the case of a Keplerian disc yields

$$\Sigma \langle v_r \rangle \frac{dj}{dr} = -\frac{1}{r} \frac{\partial}{\partial r} (r \langle F_r \rangle), \quad (4)$$

where  $v_r$  is the radial velocity in the disc and  $\Sigma = \int_{-H}^H \rho dz$  is the surface mass density. The vertical average for a quantity  $\mathcal{Q}$  is defined by

$$\langle \mathcal{Q} \rangle = \frac{\int_{-H}^H \rho \mathcal{Q} dz}{\int_{-H}^H \rho dz}. \quad (5)$$

We assume  $\mathbf{F}$  vanishes on the disc boundaries ensuring that the total angular momentum of the disc is conserved. We comment that this implies that angular momentum loss through winds or gain through mass infall is neglected. The radial angular momentum flux arising from viscosity is given by

$$F_r = -r^2 \rho \nu \frac{d\Omega}{dr}, \quad (6)$$

and thus

$$\langle F_r \rangle = -r^2 \langle \nu \rangle \Sigma \frac{d\Omega}{dr}, \quad (7)$$

For a Keplerian disc the angular velocity decreases outwards so that the angular momentum flux is directed outwards as required in order that mass accretion may occur.

Using equation (7) in equation (4) and solving for  $\langle v_r \rangle$  gives

$$\langle v_r \rangle = \frac{1}{r\Sigma} \left( \frac{dj}{dr} \right)^{-1} \frac{\partial}{\partial r} \left( r^3 \langle \nu \rangle \Sigma \frac{d\Omega}{dr} \right).$$

For a Keplerian disc in which  $j = \sqrt{GM_* r}$ , we get

$$\langle v_r \rangle = -\frac{3}{r^{1/2}\Sigma} \frac{\partial}{\partial r} \left( r^{1/2} \langle \nu \rangle \Sigma \right). \quad (8)$$

Thus the radial velocity in the disc is determined in terms of the kinematic viscosity. For a steady state disc in which  $\langle \nu \rangle \Sigma$  is constant, we find

$$\langle v_r \rangle = -\frac{3\langle \nu \rangle}{2r}.$$

This velocity is negative, consistent with accretion onto the central object.

To obtain a general equation governing the disc, the velocity (8) is used together with the vertically averaged continuity equation

$$\frac{\partial \Sigma}{\partial t} + \frac{1}{r} \frac{\partial}{\partial r} (\Sigma r \langle v_r \rangle) = 0.$$

The global evolution of the disc is thus found to be governed by a single diffusion equation for the surface density which takes the form (Lynden-Bell & Pringle 1974)

$$\frac{\partial \Sigma}{\partial t} = \frac{3}{r} \frac{\partial}{\partial r} \left( r^{1/2} \frac{\partial}{\partial r} \left( \Sigma \langle \nu \rangle r^{1/2} \right) \right). \quad (9)$$

According to this the characteristic evolution timescale for the disc will be the global diffusion timescale. The diffusion coefficient is  $3\langle \nu \rangle$  and, adopting a characteristic radius  $r$ , the global diffusion timescale is

$$t_e = \frac{r^2}{3\langle \nu \rangle}.$$

For viscosity coefficient  $\nu$ , parameterized through the  $\alpha$  prescription so that  $\nu = \alpha c_s^2 / \Omega \sim \alpha H^2 \Omega$ , we obtain

$$t_e \Omega = (1/3)(r/H)^2 \alpha^{-1}.$$

For a protostellar disc of size 100 AU with  $H/r \sim 0.1$ , and a central solar mass, we find  $t_e = 5 \times 10^5 (0.01/\alpha)$  yr. This gives lifetimes comparable to those estimated for discs around T Tauri stars if  $\alpha \sim 10^{-3}$ – $10^{-2}$ .

Equation (9) enables the evolution of the disc to be determined if  $\langle \nu \rangle$  is specified as a function of  $\Sigma$ . This can be done by solving for the vertical structure of the disc.

## 4. Vertical structure calculations

### 4.1. Basic equations

We adopt the equation of vertical hydrostatic equilibrium:

$$\frac{1}{\rho} \frac{\partial P}{\partial z} = -\Omega^2 z, \quad (10)$$

and the energy equation, which states that the rate of energy removal by radiation is locally balanced by the rate of energy production by viscous dissipation:

$$\frac{\partial \mathcal{F}}{\partial z} = \frac{9}{4} \rho \nu \Omega^2, \quad (11)$$

where  $\mathcal{F}$  is the radiative flux of energy through a surface of constant  $z$  which is given by:

$$\mathcal{F} = \frac{-16\sigma T^3}{3\kappa\rho} \frac{\partial T}{\partial z}. \quad (12)$$

Here  $P$  is the pressure,  $T$  is the temperature,  $\kappa$  is the opacity, which in general depends on both  $\rho$  and  $T$ , and  $\sigma$  is the Stefan–Boltzmann constant.

To close the system of equations, we relate  $P$ ,  $\rho$  and  $T$  through the equation of state of an ideal gas:

$$P = \frac{\rho k T}{\mu m_H}, \quad (13)$$

where  $k$  is the Boltzmann constant,  $\mu$  is the mean molecular weight and  $m_H$  is the mass of the hydrogen atom. Since the main component of protostellar disks at the temperatures we consider is molecular hydrogen, we take  $\mu = 2$ . We denote the isothermal sound speed by  $c_s$  ( $c_s^2 = P/\rho$ ).

As above, we adopt the  $\alpha$ -parametrization of Shakura & Sunyaev (1973), so that the kinematic viscosity is written  $\nu = \alpha c_s^2 / \Omega$ . In general,  $\alpha$  is a function of both  $r$  and  $z$ . However, we shall limit our calculations presented below to cases with constant  $\alpha$ . With this formalism, equation (11) becomes:

$$\frac{\partial \mathcal{F}}{\partial z} = \frac{9}{4} \alpha \Omega P. \quad (14)$$

*Boundary conditions* We have to solve three first order ordinary differential equations for the three variables  $\mathcal{F}$ ,  $P$  (or equivalently  $\rho$ ), and  $T$  as a function of  $z$  at a given radius  $r$ . Accordingly, we need three boundary conditions at each  $r$ . We shall denote with a subscript  $s$  values at the disk surface.

The first boundary condition is obtained by integrating equation (11) over  $z$  between  $-H$  and  $H$ . Since by symmetry  $\mathcal{F}(z = 0) = 0$ , this gives:

$$\mathcal{F}_s = \frac{3}{8\pi} \dot{M}_{st} \Omega^2, \quad (15)$$

where we have defined  $\dot{M}_{st} = 3\pi \langle \nu \rangle \Sigma$ . If the disk were in a steady state,  $\dot{M}_{st}$  would not vary with  $r$  and would be the constant accretion rate through the disk. In general however, this quantity does depend on  $r$ .

The second boundary condition is determined by the fact that very close to the surface of the disc, since the optical depth  $\tau_{ab}$  above the disc is small, we have:

$$P_s = g_s \tau_{ab} / \kappa_s.$$

This condition is familiar in stellar structure (e.g. Schwarzschild 1958). Using  $g_s = \Omega^2 H$ , we thus obtain

$$P_s = \frac{\Omega^2 H \tau_{ab}}{\kappa_s}. \quad (16)$$

Provided  $\tau_{ab} \ll 1$ , the results do not depend on the value of  $\tau_{ab}$  we choose (see below).

The third boundary condition we use is

$$2\sigma (T_s^4 - T_b^4) - \frac{9\alpha k T_s \Omega}{8\mu m_H \kappa_s} - \frac{3}{8\pi} \dot{M}_{st} \Omega^2 = 0. \quad (17)$$

Here the disc is assumed immersed in a medium with background temperature  $T_b$ . The surface opacity  $\kappa_s$  in general depends on  $T_s$  and  $\rho_s$  and we have used  $c_s^2 = kT/(\mu m_H)$ .

The boundary condition (17) is the same as that used by Levermore & Pomraning (1981) in the Eddington approximation (their eq. [56] with  $\gamma = 1/2$ ). In the simple case when  $T_b = 0$ , and the surface dissipation term involving  $\alpha$  is set to zero, it simply relates the disc surface temperature to the emergent radiation flux.

*Disc models* At a given radius  $r$  and for a given values of the parameters  $\dot{M}_{st}$  and  $\alpha$ , we solve equations (10), (12) and (14) with the boundary conditions (15), (16) and (17) to find the dependence of the state variables on  $z$ . The opacity is taken from Bell & Lin (1994). This has contributions from dust grains, molecules, atoms and ions. It is written in the form  $\kappa = \kappa_i \rho^a T^b$  where  $\kappa_i$ ,  $a$  and  $b$  vary with temperature.

The equations are integrated using a fifth-order Runge-Kutta method with adaptive step length (Press et al. 1992). For a specified  $\dot{M}_{st}$ , we determine the value of  $H$ , the vertical height of the disc surface. This is done iteratively. Starting from an estimated value of  $H$ , after satisfying the surface boundary conditions, the equations are integrated down to the mid-plane  $z = 0$ . The condition that  $\mathcal{F} = 0$  at  $z = 0$  will not in general be satisfied. An iteration procedure (e.g. the Newton-Raphson method) is used to adjust value of  $H$  until  $\mathcal{F} = 0$  at  $z = 0$  to a specified accuracy.

An important point to note is that as well as finding the disc structure, we also determine the surface density  $\Sigma$  for a given  $\dot{M}_{st} = 3\pi\langle\nu\rangle\Sigma$ . Thus a  $\langle\nu\rangle, \Sigma$  relation is derived.

In the calculations presented here, we have taken the optical depth of the atmosphere above the disk surface  $\tau_{ab} = 10^{-2}$  and a background temperature  $T_b = 10$  K. In these calculations the temperatures are lower than about 4,000 K, so that, at the densities we consider, hydrogen is not dissociated and the mean molecular weight  $\mu = 2$ .

In the optically thick regions of the disk, the value of  $H$  is independent of the value of  $\tau_{ab}$  we choose. However, this is not the case in optically thin regions where we find that, as expected, the smaller  $\tau_{ab}$ , the larger  $H$ . However, this dependence of  $H$  on  $\tau_{ab}$  has no physical significance, since in all cases, the mass is concentrated towards the disk mid-plane in a layer with thickness independent of  $\tau_{ab}$ .

For example, for  $\dot{M}_{st} = 10^{-8} M_{\odot} \text{ yr}^{-1}$  and  $\alpha = 10^{-2}$ , we find, at  $r = 100$  AU, that  $H/r = 0.08$  and  $0.24$  for  $\tau_{ab} = 10^{-2}$  and  $10^{-5}$ , respectively. However, in both cases, the surface density, the optical thickness and the mid-plane temperature are the same. Only the mid-plane pressure varies slightly (by about 30%) between these cases.

In Figures 1a–c, we plot  $H/r$ ,  $\Sigma$  and the mid-plane temperature  $T_m$  versus  $r$  for  $\dot{M}_{st}$  between  $10^{-9}$  and  $10^{-6} M_{\odot}/\text{year}$  (assuming this quantity is the same at all radii, i.e. the disk is in a steady state) and for illustrative purposes we have adopted  $\alpha = 10^{-3}$ .

Figure 1a indicates that the outer parts of the disk are shielded from the radiation of the central star by the inner parts. This is in agreement with the results of Lin & Papaloizou (1980) and Bell et al. (1997). For  $\alpha = 10^{-3}$ , the radius beyond which the disk is not illuminated by the central star varies from 0.2 AU to about 3 AU when  $\dot{M}_{st}$  goes from  $10^{-9}$  to  $10^{-6} M_{\odot} \text{ yr}^{-1}$ . These values of the radius move to 0.1 and 2 AU when  $\alpha = 10^{-2}$ . Since reprocessing of the stellar radiation by the disk is not an important heating factor below these radii, this process will in general not be important in protostellar disks. We note that this result is independent of the value of  $\tau_{ab}$  we have taken. Indeed, as we pointed out above, only the thickness of the optically thin parts of the disk (which do not reprocess any radiation) gets larger when  $\tau_{ab}$  is decreased.

The values of  $H/r$ ,  $\Sigma$  and  $T_m$  we get are qualitatively similar to those obtained by Lin & Papaloizou (1980), who adopted a prescription for viscosity based on convection, and Bell et al. (1997). Our values of  $H/r$  are somewhat larger though, since  $H$  is measured from the disk mid-plane to the surface such that  $\tau_{ab}$  is small, and not  $2/3$  as usually assumed. However, as we commented above, this has no effect on the other physical quantities. We also recall that  $H$ , as defined here, is about 2–3 times larger than  $c_s/\Omega$ , with  $c_s$  being the mid-plane sound speed, which is often used to define the disc semi-thickness.

*Time dependent evolution of the disc* We determine the evolution of the radial structure of a non-steady  $\alpha$ -disk by solving the diffusion equation (9). To do this, we need to use the relation between  $\dot{M}_{st} = 3\pi\langle\nu\rangle\Sigma$  and  $\Sigma$  at each radius. Interpolation of or piece-wise power law fits to numerical data may be used to

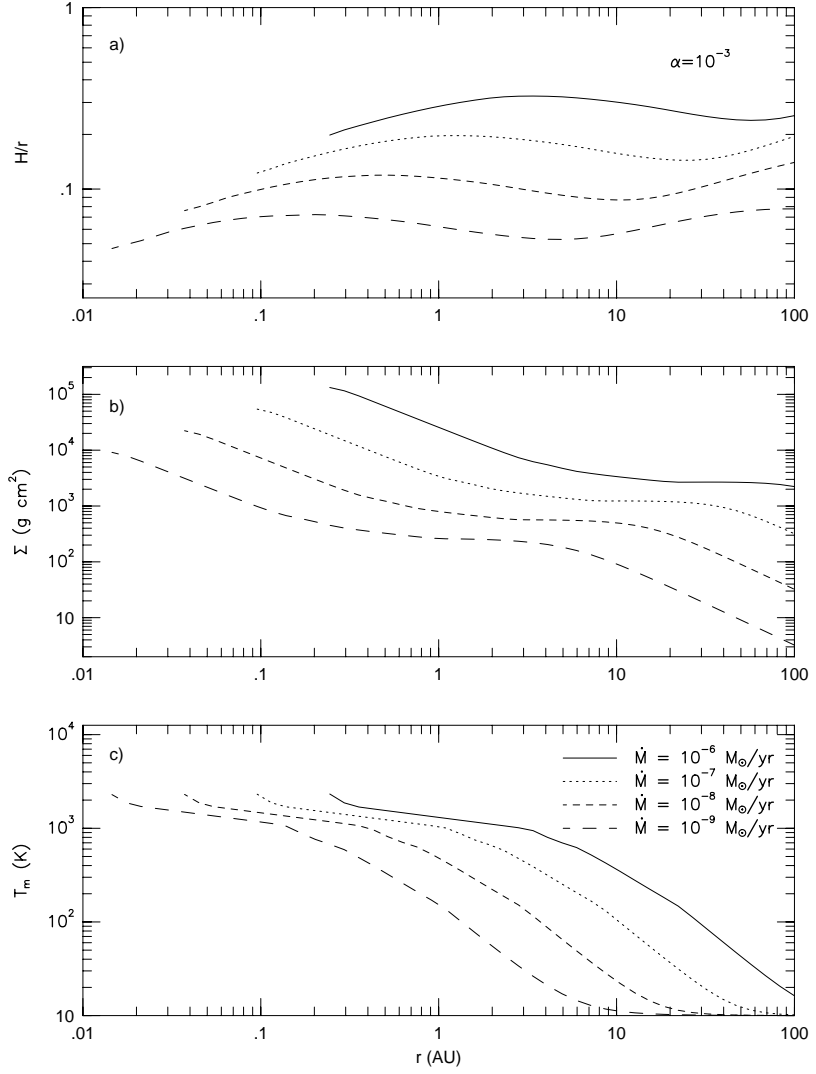


Figure 1. Shown is  $H/r$  (plot a),  $\Sigma$  in units  $\text{g cm}^{-2}$  (plot b) and  $T_m$  in K (plot c) vs.  $r/\text{AU}$  using a logarithmic scale for  $\dot{M}_{st}$  (in units  $M_{\odot} \text{ yr}^{-1}$ ) =  $10^{-6}$  (solid line),  $10^{-7}$  (dotted line),  $10^{-8}$  (short-dashed line) and  $10^{-9}$  (long-dashed line) and for  $\alpha = 10^{-3}$ .

represent this relation and more details of these will be published elsewhere. We note that they can be used either to compute  $\Sigma$  from  $\dot{M}_{st}$  or  $\dot{M}_{st}$  from  $\Sigma$ .

In Figures 2a–b we plot both the curves  $\dot{M}_{st}(\Sigma)$  that we get from the vertical structure integrations as described above and those obtained from piece-wise power law fits. Figures 2a and 2b are for  $\alpha = 10^{-2}$  and  $10^{-3}$ , respectively. In each case the radius varies between 0.01 and 100 AU. If we calculate  $\dot{M}_{st}$  using the fits with  $\Sigma$  as an input parameter, the average error is 22, 18, 13% and the maximum error is 55, 48, 42% for  $\alpha = 10^{-4}, 10^{-3}$ , and  $10^{-2}$ , respectively. We see that the fits give a good approximation.

Using the  $(\dot{M}_{st}, \Sigma)$  relation derived from the integrations, we solved equation (9) using explicit finite difference techniques. We considered the situation of a disc with initially  $0.1 M_{\odot}$  for which  $\Sigma \propto r^{-1}$ , extending to 100 AU. The central star had  $M_* = 1 M_{\odot}$  and for illustrative purposes we adopted  $\alpha = 10^{-2}$ .

In Figure 3 we show the evolution of  $\Sigma$  as a function of time. After a time  $\sim 10^6$  yr, the  $\Sigma$  profile resembles that of a steady disc in the inner parts justifying the assumption of a steady state disc model. After this time, the model is similar to that assumed for the primordial solar nebula with  $\Sigma \sim 200 \text{ g cm}^{-2}$  at 5 AU.

## 5. Planetesimal dynamics

It is thought that planetesimals can be built up from  $\mu\text{m}$  sized particles through processes of collision, sticking and accumulation occurring in a gaseous medium with some degree of turbulence (see the review by Weidenschilling & Cuzzi 1993). If physical parameters are favourable, particles with a size distribution ranging up to  $\sim$  a few km can be produced on timescales on the order of  $10^4$  yr at 1AU. The efficiency of these processes are very uncertain depending as they do on sticking probabilities and the degree of particle settling in a turbulent medium etc. Planetesimal formation efficiency may be a function of the nebula location, being more effective beyond a few AU, where ice has condensed. Here we assume that planetesimals with mass  $m_p \sim 10^{18}$  g may form on a sufficiently rapid timescale anywhere in the nebula.

We suppose the planetesimals have number distribution  $n(m) \propto m^{-q}$ , for some index  $q$ . Here the number of planetesimals in the mass range  $(m, m + dm)$  is  $n(m)dm$ . Then most of the mass is distributed in the most/least massive objects according as  $q < 2$  or  $q > 2$ . The surface density of matter in the form of planetesimals is  $\Sigma_p$ . The characteristic number density,  $N(m_p)$ , for characteristic mass  $m_p$  is then  $\Sigma_p/(2m_ph_p)$ . Here  $h_p$  is the scale height of the distribution ( $\sim \sqrt{2\pi/3} \bar{v}/\Omega$ ), where  $\bar{v}$  is the root mean square velocity dispersion.

For the typical values,  $\Sigma_p = 1 \text{ g cm}^{-2}$ ,  $m_p = 10^{21}$  g, and  $h_p = 10^{12}$  cm, the mean distance between planetesimals is  $\sim 10^{11}$  cm. This suggests use of a local box model (e.g. Stewart & Wetherill 1988). In this box, the centre of which is in circular orbit with the local keplerian angular velocity, planetesimals are assumed to move between encounters with constant velocity. In this respect, the effect of the central mass is ignored, and the planetesimals are treated using the methods of kinetic theory. The idea (Safronov 1966) is that the velocity dispersion of the planetesimals is increased by gravitational scattering, enhancing direct collisions between them through which they accumulate and grow.

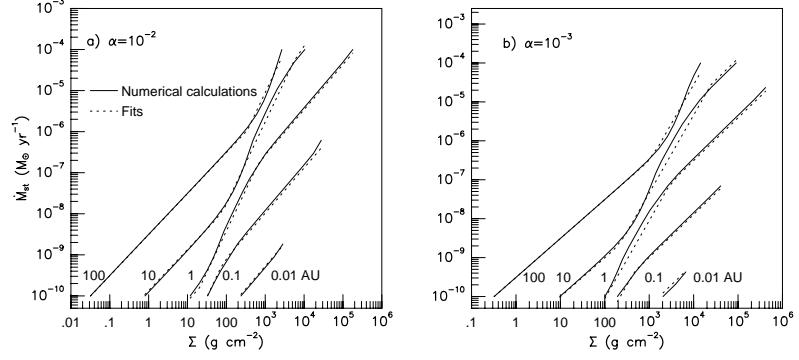


Figure 2.  $\dot{M}_{st}$  in units  $M_{\odot} \text{ yr}^{-1}$  vs.  $\Sigma$  in units  $\text{g cm}^{-2}$  using a logarithmic scale for  $\alpha = 10^{-2}$  (plot a) and  $10^{-3}$  (plot b). Both the curves corresponding to the numerical calculations (solid line) and the fits (dashed line) are shown. The label on the curves represents the radius, which varies between 0.01 and 100 AU.

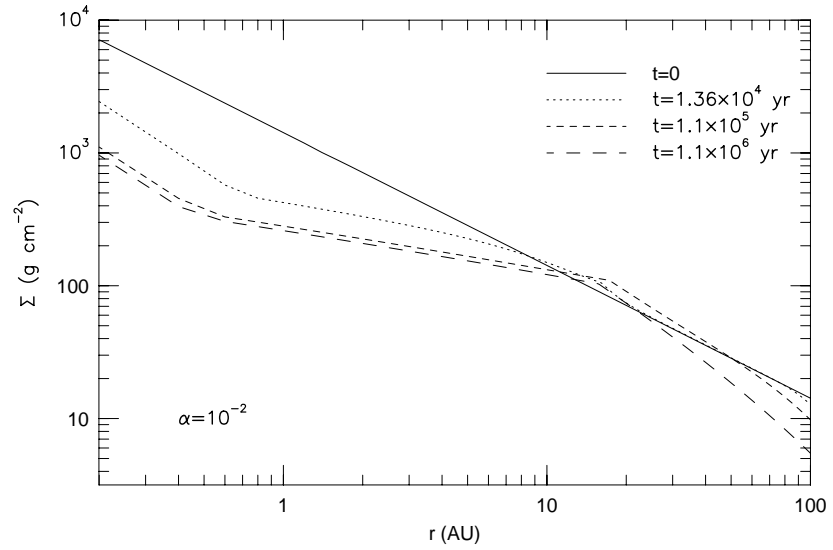


Figure 3. Solution of the diffusion equation. Shown is  $\Sigma$  in units  $\text{g cm}^{-2}$  vs.  $r$  in AU using a logarithmic scale plotted at times  $t = 0$  (solid line),  $t = 1.36 \times 10^4$  yr (dotted line),  $t = 1.1 \times 10^5$  yr (short-dashed line) and  $t = 1.1 \times 10^6$  yr (long-dashed line). This run has  $\alpha = 10^{-2}$ . The total disc mass decreases because of accretion onto the central object

The local box model fails when the largest planetesimals become isolated. That happens when accumulation has reached the stage where there are so few that they are in non-overlapping near circular orbits such that they cannot perturb similar mass objects in neighbouring orbits into collision. In this situation the central mass can no longer be neglected. To get an approximate idea of when isolation occurs at radius  $r$ , equate

$$\Sigma_p = \frac{m_p}{8\pi(m_p/M_*)^{1/3}r^2}.$$

This is a statement that there is one object in an annulus of width equal to four times its Roche lobe size. Then

$$m_p = (8\pi\Sigma_p r^2)^{3/2}(M_*)^{-1/2}.$$

This gives  $m_p = 10^{27}$  g at 5 AU for  $\Sigma_p = 1$  g cm $^{-2}$  and  $M_* = 1 M_\odot$  with obvious scalings to other surface densities and radii. Thus on the order of  $1 M_\oplus$  may be obtained at 5AU. This argument assumes circular orbits which is probably reasonable for the largest objects which are circularized through dynamical friction. After the isolation stage, planetesimal evolution is probably best followed by global N-body methods (e.g. Aarseth et al. 1993). In the gas free case the ultimate result is expected to be the formation of terrestrial planets.

### 5.1. Gravitational scattering and velocity dispersion

For a member of a swarm of equal masses interacting gravitationally, the cross section for elastic scattering is on average larger than that for a direct collision, so long as the velocity dispersion is less than the escape velocity. Thus when the velocity dispersion of the swarm is initially small, it will increase because of the effect of elastic scatterings.

The interaction radius for two masses  $m_p$  to give significant scattering is  $r_x = 2Gm_p/\bar{v}^2$ . The time between encounters is then  $t_c = 1/(N(m_p)\pi r_x^2 \bar{v} \log(\Lambda))$ . Here the  $\log(\Lambda) \sim 10$  term accounts for more distant collisions (Binney & Tremaine 1987). Using the above, one gets

$$t_c = \frac{\bar{v}^3}{4\pi N(m_p)G^2 m_p^2 \log(\Lambda)} = \sqrt{\frac{3}{2\pi}} \frac{3}{40\pi^2} \left(\frac{h_p}{r}\right)^4 \frac{M_*^2}{m_p \Omega \Sigma_p r^2}.$$

For  $m_p = 10^{20}$  g,  $\Sigma_p = 1$  g cm $^{-2}$  and  $M_* = 1 M_\odot$ , one finds at 1 AU that  $t_c = 2 \times 10^{17} (h_p/r)^4$  yr.

Note that  $h_p$  is small because the planetesimal dispersion velocities are expected to reach the escape velocity for the characteristic mass at a maximum. At this point inelastic physical impacts become as important as scattering and damp the random motions. Then for  $m_p = 10^{20}$  g,  $\bar{v} = 1.7 \times 10^3$  cm s $^{-1}$ ,  $h_p/r = 8 \times 10^{-4}$  and  $t_c \sim 9 \times 10^4$  yr at 1 AU.

Thus early planetesimal build up occurs on a rapid timescale.

### 5.2. Runaway Accretion

From the above arguments, the collision time of  $m_p$  with  $m_{p'}$  is inversely proportional to  $N(m_{p'})(m_p + m_{p'})^2$ . If this does not decrease with  $m_{p'}$ , then collisions

with larger masses are dominant and we expect velocity dispersions to build up to the escape velocity of the largest body (Safronov 1966). This occurs for  $q < 2$ .

For  $q > 2$ , the largest bodies collide with predominantly smaller ones and are circularized by dynamical friction. They can then accrete efficiently from the smaller ones which move with a velocity dispersion small compared to the escape velocity from them.

The accretion rate from planetesimals with mass  $m_{p'}$  and velocity dispersion  $\bar{v}_{p'}$  is enhanced by gravitational focusing. Thus the growth of the largest mass  $m_p$  say, with radius  $R_p$  is given by

$$\frac{dm_p}{dt} = N(m_{p'})m_{p'}\pi R_p^2\bar{v}_{p'} \left( 1 + \frac{2Gm_p}{R_p\bar{v}_{p'}^2} \right).$$

Runaway is caused both by the increase of  $R_p$  with  $m_p$  and the gravitational focusing term in brackets. The timescale for growth to isolation mass is comparable to the encounter time,  $t_c$ , indicated above. But note that growth may be slowed down through the effect of encounters between neighbouring runaways producing an increase in the velocity dispersion that propagates to all components of the system (Ida & Makino 1993)

## 6. Giant planet formation

After a solid protoplanetary core grows to a critical mass of around a few  $M_{\oplus}$ , the surrounding gaseous atmosphere can no longer grow quasi-statically in mass along with it. A process of collapse ensues possibly leading to dynamical accretion and mass growth to values characteristic of giant planets. We review the theory of this below. Such a critical core mass model is supported by the indication from models of Jupiter that it has a solid core of  $\sim 5\text{--}15 M_{\oplus}$  (Podolak et al. 1993).

### 6.1. Basic equations governing a protoplanetary envelope

Let  $\varpi$  be the spherical polar radius in a frame with origin at the centre of the planet's core. We neglect the rotation of the planet around both its own spin axis and the disc spin axis. We assume that the envelope is in hydrostatic equilibrium and spherically symmetric, so that:

$$\frac{dP}{d\varpi} = -g\rho, \tag{18}$$

where  $g = GM/\varpi^2$  is the acceleration due to gravity,  $M(\varpi)$  being the mass contained in the sphere of radius  $\varpi$  (this includes the core mass if  $\varpi$  is larger than the core radius). Mass conservation gives:

$$\frac{dM}{d\varpi} = 4\pi\varpi^2\rho. \tag{19}$$

The thermodynamic variables in the protoplanet envelope are such that the equation of state of an ideal gas does not normally apply. Here we adopt the state-of-the-art Chabrier et al. (1992) equation of state for a hydrogen and

helium mixture. We fix the abundances of hydrogen and helium to be 0.7 and 0.28 respectively.

The equation of radiative transport is:

$$\frac{dT}{d\varpi} = \frac{-3\kappa\rho}{16\sigma T^3} \frac{L}{4\pi\varpi^2}, \quad (20)$$

where  $L$  is the luminosity carried by radiation. Denoting the radiative and adiabatic temperature gradients by  $\nabla_{rad}$  and  $\nabla_{ad}$  respectively, we have

$$\nabla_{rad} = \left( \frac{\partial \ln T}{\partial \ln P} \right)_{rad} = \frac{3\kappa L_{core} P}{64\pi\sigma G M T^4}, \quad (21)$$

and

$$\nabla_{ad} = \left( \frac{\partial \ln T}{\partial \ln P} \right)_s, \quad (22)$$

with the subscript  $s$  meaning that the derivative has to be evaluated at constant entropy.

We assume that the only energy source comes from the core which outputs the core luminosity  $L_{core}$ , given by:

$$L_{core} = \dot{M}_{core} \frac{G M_{core}}{r_{core}}, \quad (23)$$

where  $M_{core}$  and  $r_{core}$  are respectively the mass and the radius of the core, and  $\dot{M}_{core}$  is the rate of accretion of planetesimals onto the core. We note that it is customary to take, instead of  $L_{core}$ , the luminosity supplied by the gravitational energy which the planetesimals entering the planet atmosphere release near the surface of the core (see, e.g., Mizuno 1980; Bodenheimer & Pollack 1986). However, when the mass of the atmosphere is small compared to that of the core, these two luminosities are comparable, providing we take for  $\dot{M}_{core}$  the rate of accretion of planetesimals onto the core during the phase of accretion of the atmosphere and not during the phase of the core formation. These two rates may be different if the core has migrated in the disk before accreting the atmosphere.

If  $\nabla_{rad} < \nabla_{ad}$ , the medium is convectively stable and the energy is transported only by radiation. In that case  $L = L_{core}$ .

When  $\nabla_{rad} > \nabla_{ad}$ , some energy is transported by convection. In that case,  $L_{core} = L + L_{conv}$ , where  $L_{conv}$  is the convective luminosity. We use the expression for  $L_{conv}$  given by mixing length theory (Cox & Giuli 1968):

$$L_{conv} = \pi\varpi^2 C_p \Lambda_{ml}^2 \left[ \left( \frac{\partial T}{\partial \varpi} \right)_s - \left( \frac{\partial T}{\partial \varpi} \right) \right]^{3/2} \sqrt{\frac{1}{2}\rho g \left| \left( \frac{\partial \rho}{\partial T} \right)_P \right|}, \quad (24)$$

where  $\Lambda_{ml} = |\alpha_{ml} P / (dP/d\varpi)|$  is the mixing length,  $\alpha_{ml}$  being a constant of order unity,  $(\partial T/\partial \varpi)_s = \nabla_{ad} T (d \ln P/d\varpi)$ , and the subscript  $P$  means that the derivative has to be evaluated for a constant pressure. The quantities  $(\partial \rho/\partial T)_P$  and  $\nabla_{ad}$  are given by Chabrier et al. (1992).

## 6.2. Boundary conditions

We suppose that the planet core has a uniform mass density  $\rho_{core}$ , here taken to be  $3.2 \text{ g cm}^{-3}$ . The core radius, which is the inner boundary of the atmosphere, is then given by:

$$r_{core} = \left( \frac{3M_{core}}{4\pi\rho_{core}} \right)^{1/3}. \quad (25)$$

The outer boundary of the atmosphere is taken to be at the Roche lobe radius  $r_L$  of the planet:

$$r_L = \frac{2}{3} \left( \frac{M_{pl}}{3M_*} \right)^{1/3} r, \quad (26)$$

where  $M_{pl} = M_{core} + M_{atm}$  is the planet mass,  $M_{atm}$  being the mass of the atmosphere, and  $r$  is the location of the planet in the disk (i.e. the separation between the planet and the central star).

To avoid confusion, we will denote the disk mid-plane temperature, pressure and mass density at the distance  $r$  from the central star by  $T_{mid}$ ,  $P_{mid}$  and  $\rho_{mid}$ , respectively.

At  $\varpi = r_L$ , the mass is equal to  $M_{pl}$ , the pressure is equal to  $P_{mid}$  and the temperature is given by:

$$T = \left( T_{mid}^4 + \frac{\tau_L L_{core}}{4\pi\sigma r_L^2} \right)^{1/4}, \quad (27)$$

where

$$\tau_L = \frac{3}{4} \kappa(\rho_{mid}, T_{mid}) \rho_{mid} r_L.$$

The condition at  $\varpi = r_{core}$  is that the mass is equal to  $M_{core}$  there.

## 6.3. Model calculations

At a given disk radius  $r$  and for a given core mass  $M_{core}$ , we solve the equations (18), (19) and (20) with the boundary conditions described above to get the structure of the envelope. The opacity law adopted was the same as that for the disk models. We note that when the density gets large, the interior of the envelope becomes convective so that the value of the opacity does not matter there.

The equations are integrated using the fifth-order Runge-Kutta method with adaptive step-size control (Press et al. 1992). We guess a starting value of  $M_{atm}$  and integrate the equations from  $\varpi = r_L$  down to the core surface  $\varpi = r_{core}$ . We then iterate the integration, adjusting  $M_{atm}$  at each step, until the solution gives  $M = M_{core}$  at  $\varpi = r_{core}$  with some accuracy.

At each radius  $r$ , for a fixed  $M_{core}$ , there is a critical core mass  $M_{crit}$  (which increases as  $M_{core}$  increases) above which no solution can be found, i.e. there can be no atmosphere in hydrostatic and thermal equilibrium confined between the radii  $r_{core}$  and  $r_L$  around cores with mass larger than  $M_{crit}$ . This is because

when the core mass is too large, the atmosphere has to collapse onto the core in order to supply adequate luminosity to support itself. For masses below  $M_{crit}$ , there are (at least) two solutions, corresponding to a low-mass and a high-mass envelope respectively.

In Figure 4 we plot  $M_{pl}$  versus  $M_{core}$  for different  $\dot{M}_{core}$  (between  $10^{-6}$  and  $10^{-11} M_{\oplus} \text{ yr}^{-1}$ ) at a radius of 5 AU and for  $T_{mid} = 140.05$  K and  $P_{mid} = 0.13 \text{ dyn cm}^{-2}$ . These values of the temperature and pressure are obtained from the vertical structure integrations described above when the parameters  $\alpha = 10^{-2}$  and  $\dot{M}_{st} = 10^{-7} M_{\odot} \text{ yr}^{-1}$  are used at  $r = 5$  AU.

The critical core mass, which decreases when  $\dot{M}_{core}$  decreases, is found to be  $22.5 M_{\oplus}$  for  $\dot{M}_{core} = 10^{-6} M_{\oplus} \text{ yr}^{-1}$  and  $2.5 M_{\oplus}$  for  $\dot{M}_{core} = 10^{-11} M_{\oplus} \text{ yr}^{-1}$ . These values are slightly larger than those found by Bodenheimer & Pollack (1986). The difference may be accounted for by the fact that we do not calculate the luminosity in exactly the same way as they do. Also we use a slightly different boundary condition for the temperature at the surface of the planet.

## 7. Disc protoplanet interaction

Once the planetary mass has attained values of around an earth mass or higher, dynamical interactions with the surrounding disc matter become important, leading to phenomena such as inward orbital migration and gap formation (Lin & Papaloizou 1993; Ward 1997; Lin et al. 1998).

Korycansky & Papaloizou (1996) considered the perturbed disc flow around an embedded protoplanet when the imposed viscosity  $\nu = 0$ . They used a shearing sheet approximation in which a patch, centered on the planet, corotating with its orbit is considered in a 2D approximation. For unit of length  $r_t = r(M_{pl}/M_*)^{1/3}$  was adopted, where  $r$  is the planet's orbital radius. We remark that  $r_t = (3^{4/3}r_L)/2$ , is a multiple of the Roche lobe radius used above. When the basic equations are expressed in dimensionless units, the only parameter defining the problem is  $\mathcal{M} = r_t/(c_s/\Omega)$ , being essentially the ratio of Roche lobe radius to disc semi-thickness.

The velocity  $\mathbf{v}$  viewed in the rotating frame was split into components involving a vortical function  $\Gamma$  and a potential  $\Phi$ :

$$\mathbf{v} = \nabla \times \hat{z}\Gamma + \nabla\Phi \quad (28)$$

For a steady flow, there is also a stream function  $\Psi$ , such that

$$\mathbf{v} = (\nabla \times \hat{z}\Psi) / \Sigma \quad (29)$$

Parameters relating to the flow for  $\mathcal{M} = 0.7$  are plotted in figures 5 and 6. Here Cartesian coordinates are adopted with origin at the centre of the protoplanet and  $x$  axis pointing along the line joining the central star to the protoplanet. The perturbed surface density (figure 5) shows trailing shock waves behind which there is a strong surface density enhancement giving rise to pronounced wakes. Also notable is the prograde disc flow around the protoplanet (figure 6). Dissipation in the shock waves, which become strong once  $\mathcal{M} > 1$ , eventually results in gap formation (Lin & Papaloizou 1993).

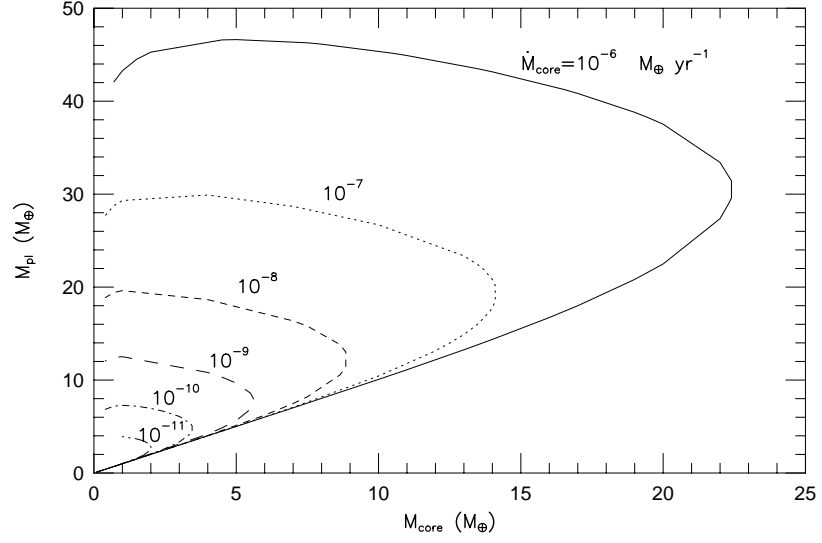


Figure 4.  $M_{pl}$  in  $M_{\oplus}$  versus  $M_{core}$  in  $M_{\oplus}$  for  $\dot{M}_{core}$  between  $10^{-6}$  and  $10^{-11} M_{\oplus} \text{ yr}^{-1}$  at a radius  $r = 5 \text{ AU}$  and for  $T_{mid} = 140.05 \text{ K}$  and  $P_{mid} = 0.13 \text{ dyn cm}^{-2}$ . From one curve to another, starting from the right,  $\dot{M}_{core}$  decreases by a factor 10. The critical core mass increases with  $\dot{M}_{core}$ , varying between  $\sim 2$  and  $22.5 M_{\oplus}$ .

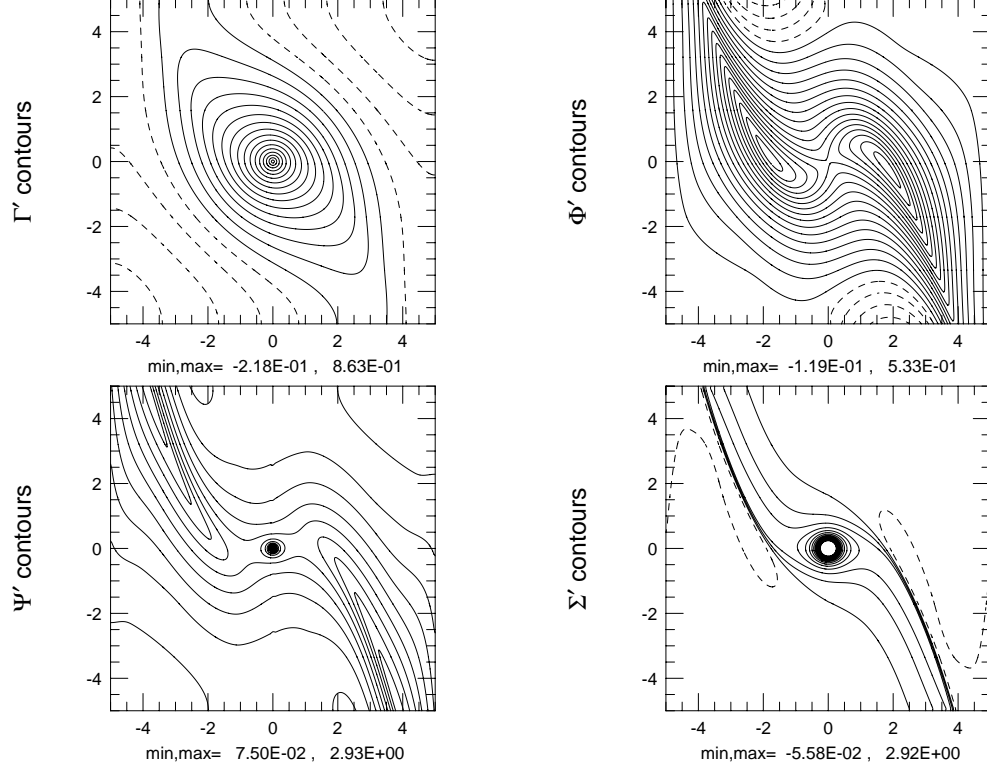


Figure 5. Flow quantities for the case  $\mathcal{M} = 0.7$  taken from Korycansky & Papaloizou (1996). Minimum and maximum contour levels plotted as indicated in the panels. Negative and maximum contour levels by dashed lines. Top left: Disturbance quantity  $\Gamma'$ , the vortical part of the velocity perturbation. Top right: Disturbance quantity  $\Phi'$ , the potential part of the velocity perturbation. Bottom left: Disturbance quantity  $\Psi'$ , the momentum stream function of the perturbed flow. Bottom right: Disturbance quantity  $\Sigma'$ , the surface density perturbation

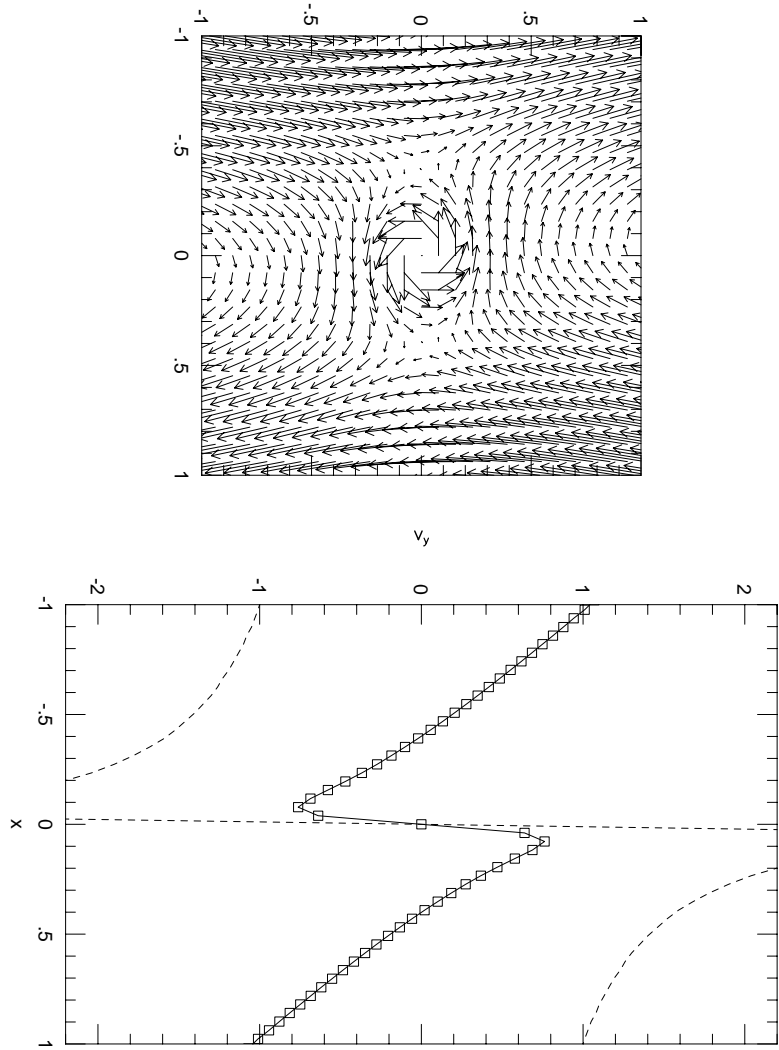


Figure 6. Velocity field (including background) near the protoplanet taken from Korycansky & Papaloizou (1996). Left: Flow field. Right: Velocity  $v_y$ , along the line  $y = 0$ .

Protoplanet–disc interaction leads to gap formation and orbital migration, which, together with tidal interaction with the central star (Terquem et al. 1998) can lead to massive planets in circular orbits, with periods of a few days, as observed (Butler et al. 1997). The reader is referred to the article by Lin et al. (1998) for an account of the dynamical phenomena which can play a role in determining the final orbital configuration of planetary systems.

## References

- Aarseth, S. J., Lin, D. N. C., & Palmer, P. L. 1993, *ApJ*, 403, 351
- Balbus, S.A. & Hawley, J. F. 1991, *ApJ*, 376, 214
- Beckwith, S. V. W., & Sargent, A. I. 1996, *Nature*, 383, 139, 144
- Bell, K. R., Cassen, P., Klahr, H. H., Henning, T. 1997, *ApJ*, 486, 372
- Bell, K. R., & Lin, D. N. C. 1994, *ApJ*, 427, 987
- Binney, J., & Tremaine, S. 1987, *Galactic Dynamics* (Princeton: Princeton Univ. Press), 3rd ed.
- Bodenheimer, P., & Pollack, J. B. 1986, *Icarus*, 67, 391
- Boss, A. P. 1998, *ApJ*, 503, 923
- Butler, R. P., Marcy, G. W., Williams, E., Hauser, H., & Shirts, P. 1997, *ApJ*, 474, L115
- Cameron, A. G. W. 1978, *Moon Planets*, 18, 5
- Chabrier, G., Saumon, D., Hubbard, W. B., & Lunine, J. I. 1992, *ApJ*, 391, 817
- Cox, J. P., & Giuli, R. T. 1968, *Principles of Stellar Structure: Physical Principles* (New York: Gordon & Breach)
- Gammie, C. F. 1996, *ApJ*, 457, 355
- Goodman, A. A., Benson, P. J., Fuller, G. A., & Myers, P. C. 1993, *ApJ*, 406, 528
- Heemskerk, M. H. M., Papaloizou, J. C. B., & Savonije, G. J. 1992, *A&A*, 260, 161
- Ida, S., & Makino, J. 1993, *Icarus*, 106, 210
- Korycansky, D. G. , & Papaloizou, J. C. B. , 1996, *ApJS*, 105, 181
- Laplace, P. S. 1796, *Exposition du Système du Monde* (Paris)
- Laughlin, G., & Bodenheimer, P. 1994, *ApJ*, 436, 335
- Levermore, C. D., & Pomraning, G. C. 1981, *ApJ*, 262, 768
- Lin, D. N. C., & Papaloizou, J. 1980, *MNRAS*, 191, 37
- Lin, D. N. C., & Papaloizou, J. 1985, in *Protostars and planets II*, ed. D. C. Black & M. S. Mathews (Tucson: Univ. Arizona Press), 981
- Lin, D. N. C., & Papaloizou, J. C. 1993, in *Protostars and planets III*, ed. E. H. Levy & J. Lunine (Tucson: Univ. Arizona Press), 749
- Lin, D. N. C., Papaloizou, J. C. B., Bryden, G., Ida, S., & Terquem, C. 1998, in *Protostars and planets IV*, ed. A. Boss, V. Mannings & S. Russel (Tucson: Univ. Arizona Press), *in press*
- Lynden–Bell, D., & Pringle, J. E. 1974, *MNRAS*, 168, 60

- McCaughrean, M. J., & Stauffer, J. R. 1994, *AJ*, 108, 1382
- Mizuno, H. 1980, *Prog. Theor. Phys.*, 64, 544
- Papaloizou, J. C. B. , & Lin, D. N. C. 1995, *ARA&A*, 33, 50
- Papaloizou, J. C., & Savonije, G. J. 1991, *MNRAS*, 248, 35
- Pickett, B. K., Cassen, P., Durisen, R. H., & Link, R. 1998, *ApJ*, 504, 468
- Podolak, M., Hubbard, W. B., & Pollack, J. B. 1993, in *Protostars and planets III*, ed. E. H. Levy & J. Lunine (Tucson: Univ. Arizona Press), 1109
- Press, W. H., Flannery, B. P., Teukolsky, S. A., & Vetterling, W. T. 1992, *Numerical Recipes: The Art of Scientific Computing* (Cambridge: Cambridge Univ. Press), 3rd ed.
- Reipurth, B., Bally, J. & Devine, D. 1997, *AJ*, 114, 2708
- Safronov, V. S. 1966, *Soviet Astron. J.* 9, 987
- Safronov, V. S. 1969, in *Evoliutsiia doplanetnogo oblaka*, Moscow
- Schwarzschild, M. 1958, *Structure and Evolution of the Stars* (Princeton: Princeton Univ. Press)
- Shakura, N. I., & Sunyaev, R. A. 1973, *A&A*, 24, 337
- Stapelfeldt, K. R., Krist, J. E., Menard, F., Bouvier, J., Padgett, D. L., & Burrows, C. J. 1998, *ApJ*, 502, 65
- Stewart, G. R. & Wetherill, G. W. 1988, *Icarus*, 74, 553
- Strom, S. E., Edwards, S., & Skrutskie, M. F. 1993, in *Protostars and planets III*, ed. E. H. Levy & J. Lunine (Tucson: Univ. Arizona Press), 837
- Terquem, C. , Papaloizou, J. C. B. , Nelson, R. P., & Lin, D. N. C. 1998, *ApJ*, 502, 788
- von Weizsäcker, C. F. 1948, *Z. Naturforsch.*, 3a, 524
- Ward, W. 1997, *Icarus*, 126, 261
- Weidenschilling, S. J., Cuzzi, J. N. 1993, in *Protostars and planets III*, ed. E. H. Levy & J. Lunine (Tucson: Univ. Arizona Press), 1031
- Wetherill, G. W., & Stewart, G. R. 1989, *Icarus*, 77, 330